

Feature Extraction of Visual Evoked Potentials Using Wavelet Transform and Singular Value Decomposition

Ahmed Almurshed^{1*}, Abd Khamim Ismail², Najwa Sulaiman³

1. Department of Physics, College of Science, Al-Muthanna University, Al-Muthanna, Iraq

2. Department of Physics, Faculty of Science, Universiti Teknologi Malaysia, Johor, Malaysia

3. Department of Medical Physics, College of Science, Al-Karkh University of Science, Baghdad, Iraq

ARTICLE INFO

ABSTRACT

Article type:

Original Article

Article history:

Received: Jan 01, 2018

Accepted: Apr 18, 2018

Keywords:

Classification
Feature Extraction
Singular Value
Decomposition (SVD)
Visual Evoked Potentials
Wavelet Transform

Introduction: Brain visual evoked potential (VEP) signals are commonly known to be accompanied by high levels of background noise typically from the spontaneous background brain activity of electroencephalography (EEG) signals.

Material and Methods: A model based on dyadic filter bank, discrete wavelet transform (DWT), and singular value decomposition (SVD) was developed to analyze the raw data of visual evoked potentials and extract time-locked signals with external visual stimulation. A bio-amplifier (iERG 100P) and data acquisition system (OMB-DAQ-3000) were utilized to record EEG raw data from the human scalp. MATLAB Data Acquisition Toolbox, Wavelet Toolbox, and Simulink model were employed to analyze EEG signals and extract VEP responses.

Results: Results were verified in Simulink environment for the real recorded EEG data. The proposed model allowed precise decomposition and classification of VEP signals through the combined operation of DWT and SVD. DWT was successfully used for the decomposition of VEP signals to different frequencies followed by SVD for feature extraction and classification.

Conclusion: The visual and quantitative results indicated that the impact of the proposed technique of combining DWT and SVD was promising. Combining the two techniques led to a two-fold increase in the impact of peak signal to noise ratio of all the tested signals compared to using each technique individually.

► Please cite this article as:

Almurshed A, Khamim Ismail A, Sulaiman N. Feature Extraction of Visual Evoked Potentials Using Wavelet Transform and Singular Value Decomposition. Iran J Med Phys 2018; 15: 206-214. 10.22038/ijmp.2018.28583.1311.

Introduction

Visual evoked potentials (VEPs) are alterations derivative of spontaneous electroencephalogram (EEG) due to external visual stimulation. They are time-locked (TL) to the presentation of stimulus. Also, they consist of a characteristic pattern of responses more or less reproducible under similar experimental circumstances [1, 2]. To understand the brain's response, different tasks, events, or sequences of stimuli can be used to investigate various sensory and cognitive functions, brain states and conditions, as well as brain disorders. In fact, VEP is an essential technique in neuroscience [3].

Amplitude of VEP signals is very lower compared to that of spontaneous EEG signals. Therefore, VEPs are embedded in the baseline of EEG. Thus, numerous sequences of trials are averaged together (grand average) to enhance the picked up response of VEP. Thus, VEPs are time-locked to checkerboard stimulation and their contributions are combined together. The overlapping of responses cancels the background EEG (the noise) [4]. One of the key parameters of VEP recording is the number of overlapped trials. Large trial number sequences help to optimize the VEP ratio, whereas they may cause some

distortions in the recorded signal due to visual illusion.

The grand average of VEPs implicate a few trial sequences, which would eventually help to extract single response of VEPs from the ongoing EEG [5, 6]. Researchers proposed several methods and algorithms in order to filter averaged VEPs. These methods are based on the digital filter design, for example, variant and invariant Wiener filters. Such methods are used to enhance the result of transient evoked response corresponding to precise temporal and spectral analyses. These filters are based on fast Fourier transform (sines and cosines signal decomposition). Therefore, there is a possibility of flaws in reconstruction.

The limitations described in the previous paragraph can be overcome by using wavelet transform, which is a time-frequency representation first proposed by Grossmann and Morlet [7]. This technique is efficiently applied to analyze EEG signals in time-frequency domains [8-10]. Wavelet analysis decomposes a signal into a specific time window by selecting an appropriate length of window [11]. However, the modulation of the time signal affects the spectrum. Real value of mother wavelets is usually symmetric and its coefficients do not carry any phase information.

*Corresponding Author: Department of Physics, College of Science, Al-Muthanna University, Al-Muthanna, Iraq. Tel: +9647740705626;
Email: fhahmed2@gmail.com

Nonetheless, Gabor filters and complex valued Morlet [12] wavelets retain phase information.

Real-time control of EEG signals has been applied in brain computer interface (BCI) [13]. Fuzzy and neural networks have been used for pattern recognition of dexterous robotic hands. The accuracy of hand movement was calculated to be nearly 100% as compared to other accompanying mental tasks [14]. EEG-based approach has also been employed for pattern recognition of complicated hand activities using DWT, ANN, and SVD, and a high recognition accuracy was achieved [15]. A 3D real-time feedback in emotional virtual environments was recognized and visualized based on fractal dimension algorithm of quantification of basic emotions on an avatar by adding "emotion dimension" to BCI [16, 17].

Steady state visual evoked potential (SSVEP) has been used recently in different applications in BCI and robotic control to assess visual acuity in normal adults [18] and control gripping of a robotic hand [19]. Studies showed that after a very short period of training, SSVEP-based BCI systems could reach very high accuracies [20]. However, BCI and control of VEP are confined to SSVEP.

In this paper, a low-cost real time EEG-based approach was proposed for transient visual evoked potentials analysis and feature extraction using DWT and SVD in MATLAB Simulink. One significant advantage of this method over traditional methods is that the VEP signal from the brain can be accurately picked up and extracted from EEG background noise and decomposed to different frequency band groups, which can then be categorized with SVD.

Materials and Methods

Wavelet transform

The integrated function of signal $f(t)$ times a set of basic functions, which are compressed or stretched and shifted versions of the "mother wavelet", known as wavelet transform (WT). A wavelet family may have several forms based on the mathematical constraints to reconstruct the original waveform after employing inverse WT.

Continuous WT (CWT) can be described as:

$$w_{a,b} = \int_{-\infty}^{\infty} f(t) \times g_{a,b}^*(t) dt \quad (1)$$

, and

$$g_{a,b}(t) = \frac{1}{\sqrt{a}} g \frac{(t-b)}{a} \quad (2)$$

where $g_{a,b}(t)$ is the mother wavelet or analyzing wavelet, $g_{a,b}^*(t)$ is its complex conjugate, t denotes time, a shows dilation (scale) parameter, and b signifies translation parameter.

The inverse WT is given as:

$$f(t) = C \iint w_{a,b} g_{a,b}(t)/a^2 da * db \quad \text{For } a > 0, \quad (3)$$

where C is the normalization constant.

The mother wavelet, $g_{a,b}(t)$, is constrained by finite energy, and the time average is equal to zero. Because of these constraints, WT removes the DC

component of the mother signal and adds it back while performing inverse WT.

WT provides an expansion for function $f(t)$ in terms of basic functions $g_{a,b}(t)$, which consist of dilation and translation of wavelet function. Equation (2) signifies that as parameter a increases, the function $g_{a,b}(t-b)$ expands along the time axis, that is, dilation and contraction of the mother wavelet is possible through varying the value of a .

If parameter b increases, the function translates (slide) along the time axis. Unlike sinusoidal basis functions, the wavelet basis functions do not have energy concentrated at a single frequency. The information of lower frequency and higher frequency ends is recorded based on the value of parameter a . For large a values, base functions are broader and energy is concentrated at lower frequencies. On the other hand, for small a values, base functions are narrower and energy is concentrated at higher frequencies. Thus, WT captures frequency information in certain frequency ranges rather than line frequencies [21].

It is well known that digital signal processing techniques work with discrete signals. Instead of continuous range of values of a and b in Equation (2), the values are restricted to a set of discrete values such that $a=2^k$ and $b=2^k m$, where k and m are integers.

These values are substituted in discrete WT (DWT) as follows:

$$w_{k,m} = \int f(t) \times g_{2^k, 2^k m}^*(t) dt \quad (4)$$

For DWT, the length of the signal must be of the order of 2^n , where n is an integer.

Singular value decomposition (SVD)

The SVD method is used as a tool in statistical analysis and data processing. The SVD of an $X(M \times N)$ matrix of the signal x is given as:

$$X = U \Sigma V^T \quad (5)$$

where $V(N \times N)$ and $U(M \times M)$ are orthonormal matrices, and Σ is an $M \times N$ diagonal matrix of singular values ($\sigma_{ij} = 0$ if $i = j$ and $\sigma_{11} \geq \sigma_{22} \geq \dots \geq \sigma_{NN}$). The matrix columns of V and U are mutually orthogonal and called the right and left singular values, respectively [10]. The matrix is composed of individual singular values (σ_{ii}), these values represent the importance of each individual value in the matrix. In other words, the singular value of large individual singular value carries more structural information of embedded patterns in the matrix than any other individual singular values [22, 23].

Participants

Ten male subjects volunteered for this experiment. Volunteers were confirmed that they were not suffering from any ophthalmological, neurological, and psychological disorders. These participants were aged 22-31 years old. The volunteers were right-handed with normal visual acuity (some were wearing spectacles and none of them was wearing contact lenses). The subjects were

informed of the study procedures and objectives and signed a consent form. The volunteers were trained to sit tight on a comfortable chair, which was 100 cm away from an LCD monitor. They were informed to reduce any body movements such as head, hands, legs, and even fingers. Blinking and yawning were also asked to be avoided as far as possible to avoid EMG artifact during EEG recording. The volunteers were required to stay attentive during VEP recording.

Experimental Setup

In this study, the EEG data were recorded from 10 normal subjects using a four-channel Bio amplifier (iERG 100P from GlobalTown Microtech, USA). The sampling rate was 1000 Hz. The frontal and occipital areas of the brain were covered in this study. The 10-20 electrode system was employed to distribute the electrodes on the scalp. The frontal (Fp1, Fp2) lobe and occipital lobe (O1, O2) were referenced to the central electrode (Cz) and grounded to the right and left earlobes. Shielded differential electrodes (EAD-AGC8S, assembled with sintered Ag/AgCl electrodes) were used to pick up the signals from the scalp. OMEGA DAQ (OMB-DAQ-3000 Series, UK) was used to acquire the recorded data for further processing.

VEP signals were obtained using visual pattern reversal checkerboard stimulation from normal subjects. The subjects were sitting on a comfortable chair (100 cm away from the LCD with 1 Hz temporal frequency and 12x16 checkerboard resolution). The subjects were instructed to focus on a red point at the center of the LCD screen.

A visual simulation software was designed using Delphi programming language, where pattern stimulation, resolution, and temporal frequency could be manipulated. In this experiment, a 1 Hz (2 reversals per sec) checkerboard pattern was chosen to stimulate the brain. A high-speed photodiode fixed at the corner of the screen connected to a preamplifier, and a comparator circuit was utilized to send pulse signal for triggering, timing, and synchronizing the DAQ. Therefore, a precise marking of the checkerboard pattern reversal could be performed for time-locked signal averaging. For monitoring purpose, pulse signals from the photodiode were fed into one of the input channels of the DAQ.

Figure 1 schematically shows the recording system for the implementation of real-time VEP system with discrete wavelet analysis, and SVD was performed using MATLAB Simulink.

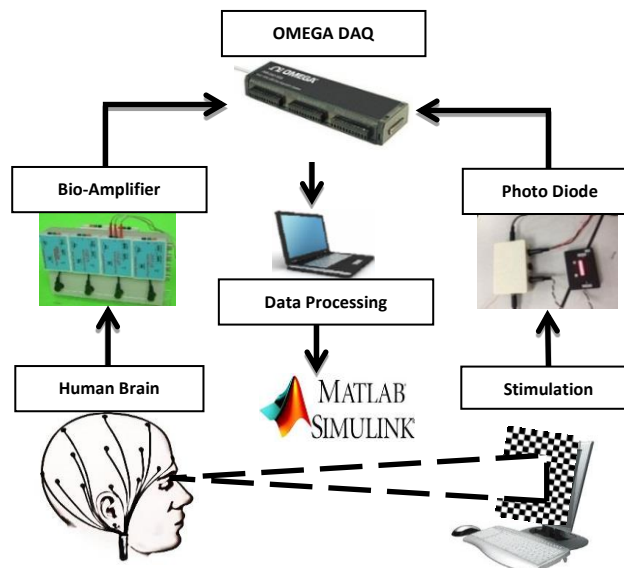


Figure 1. Schematic diagram of the experimental setup: checkerboard stimulation synchronized using photodiode with four-channel iERG 100P bio-amplifier from GlobalTown Microtech, and signal recording and data acquiring with OMB-DAQ-3000 Series

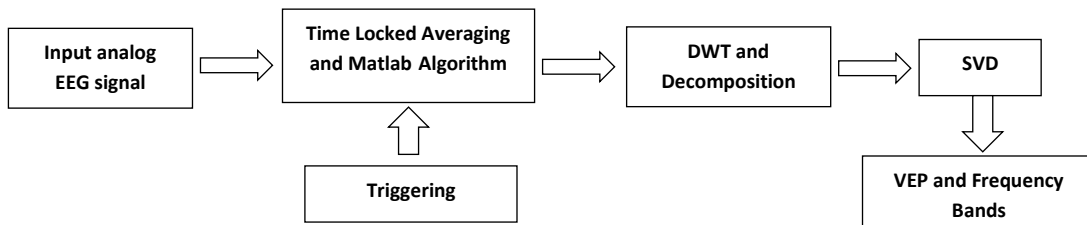


Figure 2. Block diagram of data processing: exporting analog data to the Simulink, time-lock averaging, discrete wavelet transformation, and singular value decomposition

Simulink and Data Processing

A 1-MHz, 16-bit OMB-DAQ-3000 Series data acquisition system was linked to MATLAB toolbox to display brain signals from four channels and another one channel of trigger signal from the photodiode in real-time on the screen. Then, the data were exported to MATLAB Simulink environment through an “analog input” for further processing and

analysis. Figure 2 shows the block diagram of data processing.

The signals from the five channels were read into the analog input block with fixed acquisition parameters. Then, the data were forwarded to MATLAB Workspace and recalled again for the following algorithm.

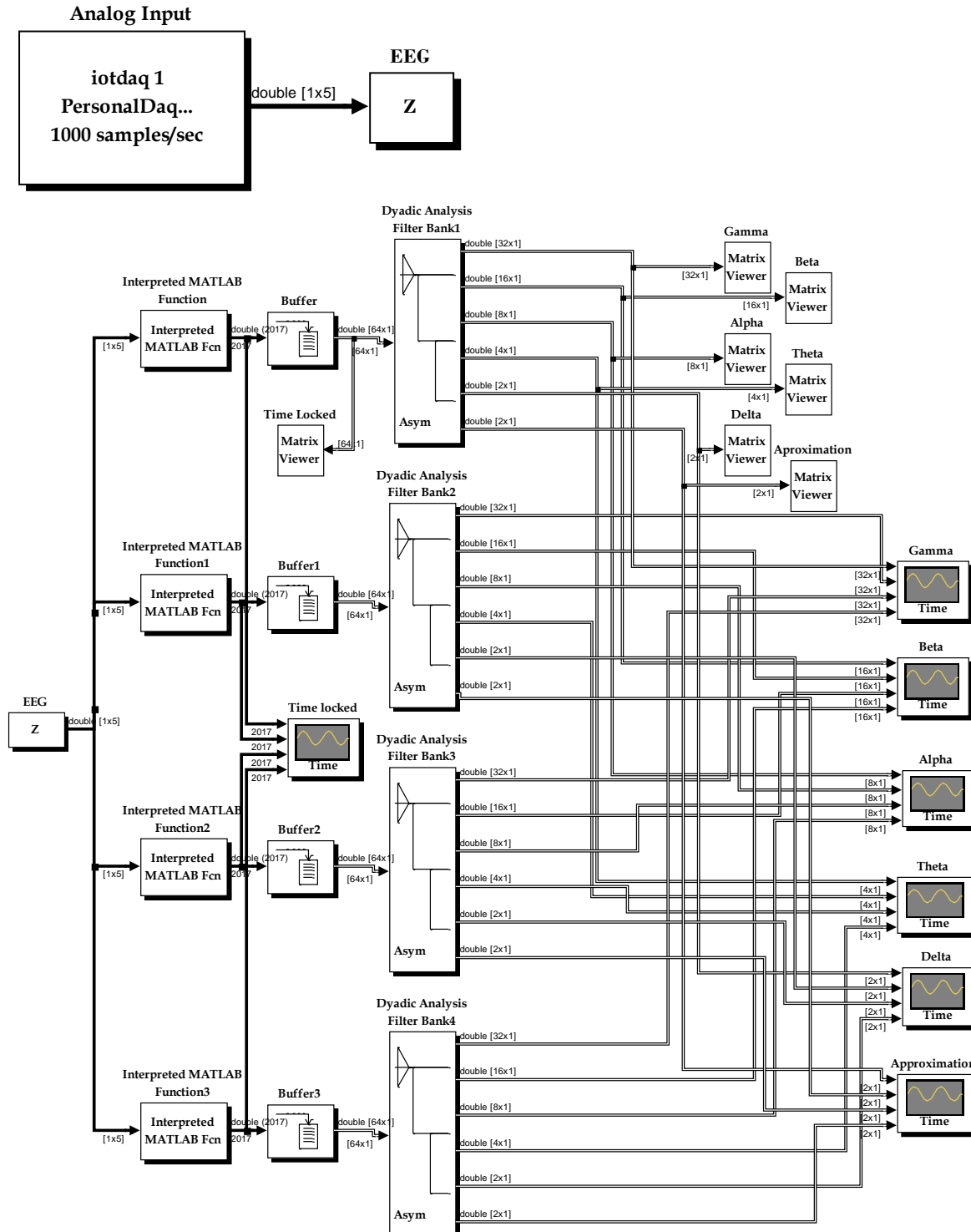


Figure 3. MATLAB Simulink model, importing the data in real-time to Simulink environment, time-lock averaging, and dyadic filter bank wavelet analysis

The algorithm detects any variation in the starting point of positive-edge-trigger signal and records this position in a new matrix. The whole process is based on the sampling rate of the recorded data. Next, the brain signals from the four channels are segmented for time-locked averaging. This algorithm is set as a functional block and interpreted and utilized by MATLAB Simulink through “interpreted MATLAB function block”.

Dyadic filter bank wavelet analysis known as “dyadic filter bank block” is applied to the signal. DWT decomposes the signal into its approximations and details. Each filter stage decomposes the signal to half of the previous stage, and accordingly, it separates unwanted signals and classifies them into different frequency bands. In the Simulink model (as shown in Figure 3), the signal becomes doubled after each stage of dyadic filter processing. “Time scope block” is used to display the signal.

The “matrix viewer block” is used to display the details of frequency at each stage, which displays the frequency and magnitude of the component in a small fraction of time.

Results

Raw signals are transferred from real-time to MATLAB Simulink analog input data acquisition toolbox. The data are processed for time-locked averaging and visual stimulation. The input data were segmented and averaged using MATLAB algorithm, which depends on its trigger. Figure 4 shows the time-lock averaging signals recorded from the left occipital area after removing EEG background from VEP response. Following the standard pattern reversal visual evoked potentials, signals are recorded from the occipital lobe; these signals consist of three main peaks. The first negative peak was at position N75 followed by a positive peak at P100, and another negative peak was at around N135 [24, 25]. The frontal negativity N100 is from the frontal lobe pattern reversal VEP [26, 27]. By time-lock averaging, the background noise is removed from the signal, while relatively small high frequency noises are retained by the signal. High frequency noise incursion within the signal is removed by applying long time wavelet window to obtain a finer low frequency resolution. This leads to precise frequency information and short wavelet time window to obtain high frequency information, and in turn, precise time information [28]. Thus, VEP provides a direct measurement of cortical activity with high temporal resolution [29].

Dyadic filter bank wavelet transforms using Daubechies wavelet (db) and decomposes signals to their details. Figure 5 shows the results of wavelet decomposition of db5 for five levels of left occipital electrode (O1). Output buffer size is set to 64, which converts sample-based signals to frame-based signals. Wavelet dyadic filter bank breaks the signal in each stage to half of the previous stage. Initially, the frame is set to 64. In the next stage, frame size is

fixed at 32. The wavelet decomposes the signal into different frequency bands of various stages of filter bank analysis.

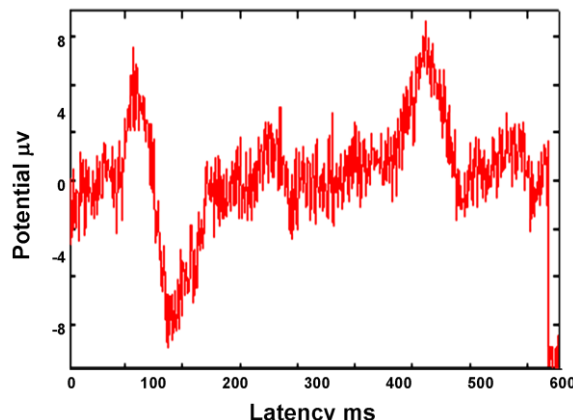


Figure 4. Time-locked signal averaging signal recorded from the left occipital electrode (O1)

The wavelet details are classified into different frequency bands (i.e., gamma, beta, alpha, theta, and delta). This can be seen in the Simulink model (Figure 3) where each time scope displays one of the frequency bands. Figure 5 displays VEP responses, the results of dyadic filter bank wavelet analysis of time-locked signal, and how effectively wavelet filter removed high-frequency noise from the signals.

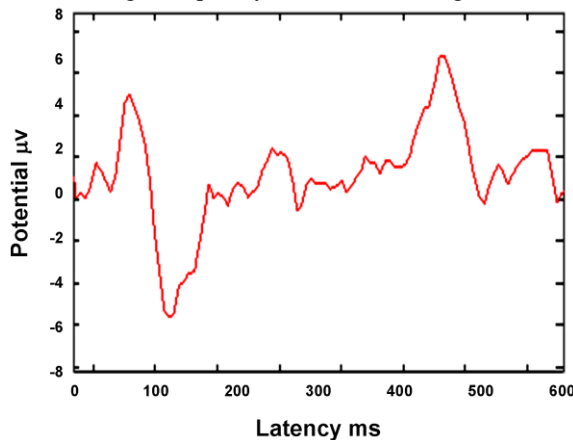
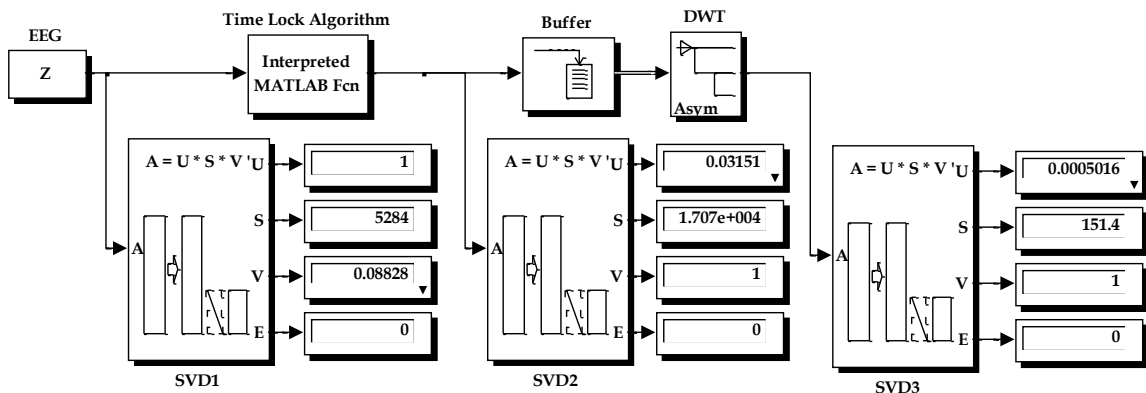


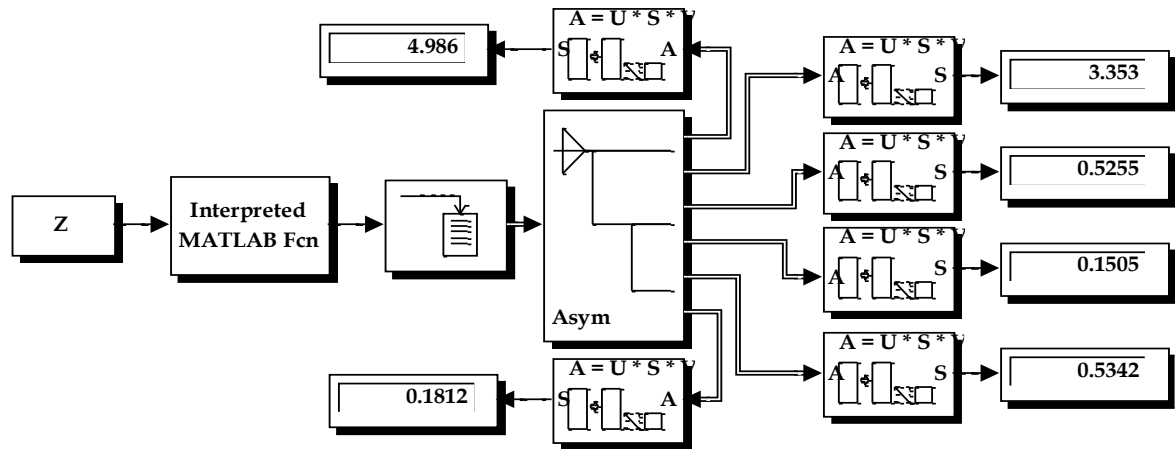
Figure 5. Discrete wavelet analysis of a signal recorded from the left occipital electrode (O1)

SVD is used in digital signal processing applications for noise reduction and future extraction. The main idea is to let a matrix X represent the noisy signal, calculate SVD, and then dismiss small singular values from X . Thus, small singular values mainly represent the noise. Figure 6(a) exhibits the block model of SVD used to classify DWT output, where the smaller values of S signify less noise signal. Furthermore, the error status port E represents singular value decomposition calculation; the possible values obtained on the port are 0 and 1, these values reflect converge and does not converge (fails to converge), respectively. SVD is applied to classify signals based on their frequency bands (details) by calculating SVD for each analyzing level as shown in Figure 6(b).

(a)



(b)

**Figure 6.** MATLAB Simulink model singular value decomposition of dyadic filter bank

Discussion

The VEP signals recorded from the occipital area of the brain are presented in figures 4 and 5. According to the International Society of Clinical Electrophysiology of Vision (ISCEV) [30], the pattern reversal checkerboard stimulation of transient VEPs consists of three peaks. The first one is negative trough appearing at 75 ms after the onset of stimulation (N75). The second one is positive peak appearing at 100 ms after the onset of stimulation (P100), and the third one is a negative trough appearing at 135 ms after the onset of stimulation (N135). The positive peak at 100 ms is usually a main peak of VEP. This peak may show reasonable differences between subjects, less within-subject interocular variation, this variation can be overcome with repeated measurements over time. The epoch of the main peak (P100) is affected by technical parameters, for example pattern stimulation size, luminance and contrast of the screen, digital filter, patient age, refractive defect of the eye, poor concentration, and excessive constriction of the pupil of the eye [25]. Thus, the proposed method extracted VEP signal in good agreement with the standard one.

In order to validate the performance of the proposed technique, peak signal to noise ratio (PSNR) is calculated for each level of wavelet analysis. Each level of decomposition represents

frequency band and the last one is the approximation. Tables 1 and 2 show the quantitative comparison of PSNR of the occipital and frontal lobes between the proposed wavelet and SVD techniques, respectively. However, Figure 7 exhibits that SVD acts as a classifier for each level of WT. Hence, it can classify decomposition levels into different frequency bands. It is clear that each band is represented by a specific value of SVD.

Figure 8 shows the advantage of the proposed method by combining both DWT and SVD. A significant improvement is observed by merging DWT and SVD, and the value of PSNR almost doubled as compare to the previous method of DWT only. There was a remarkable improvement in the value of PSNR in the approximation. While a slight improvement was noticed in the details. This is logical since very little information is available in each detail (level of analysis) for frequency bands.

Table 1. Singular value decomposition (SVD) and peak signal to noise ratio for wavelet transform and SVD in the occipital lobe

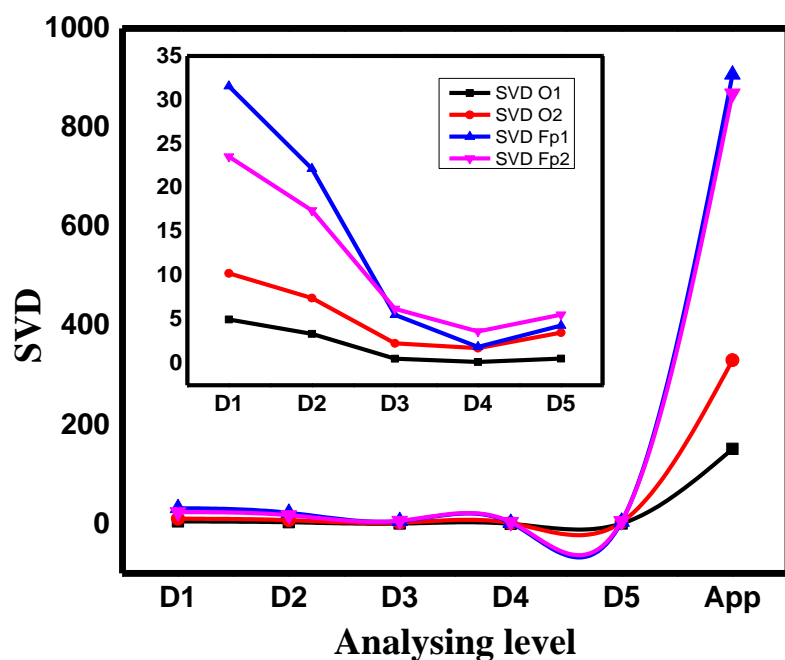
Analysis Level	O1			O2		
	SVD	PSNR-DWT	PSNR-SVD	SVD	PSNR-DWT	PSNR-SVD
D1	4.986	18.77	32.73	10.25	1.932	22.15
D2	3.353	11.76	22.26	7.432	6.496	23.92
D3	0.5255	11.41	17	2.277	10.16	17.31
D4	0.1505	2.062	18.51	1.721	2.968	7.683
D5	0.5342	2.155	7.601	3.49	-8.821	2.037
App	151.4	-40.57	3.033	330.3	-47.27	3.105

SVD: Singular value decomposition PSNR: peak signal to noise ratio DWT: discrete wavelet transform

Table 2. The singular value decomposition (SVD) and peak signal to noise ratio (PSNR) for discrete wavelet transform and SVD in the frontal lobe

Analysis Level	Fp1			Fp2		
	SVD	PSNR-DWT	PSNR-SVD	SVD	PSNR-DWT	PSNR-SVD
D1	31.56	-3.397	26.58	23.54	-0.1174	27.32
D2	22.15	5.034	31.94	17.4	8.052	32.86
D3	5.52	2.007	16.85	6.195	-8.827	7.013
D4	1.868	14.41	19.84	3.621	-5.334	5.843
D5	4.297	-2.785	9.878	5.537	6.508	21.37
App	906.9	-56.1	3.052	868.8	-55.71	3.073

SVD: Singular value decomposition PSNR: peak signal to noise ratio DWT: discrete wavelet transform

**Figure 7.** Comparisons of singular value decomposition values of the signals for different wavelet levels

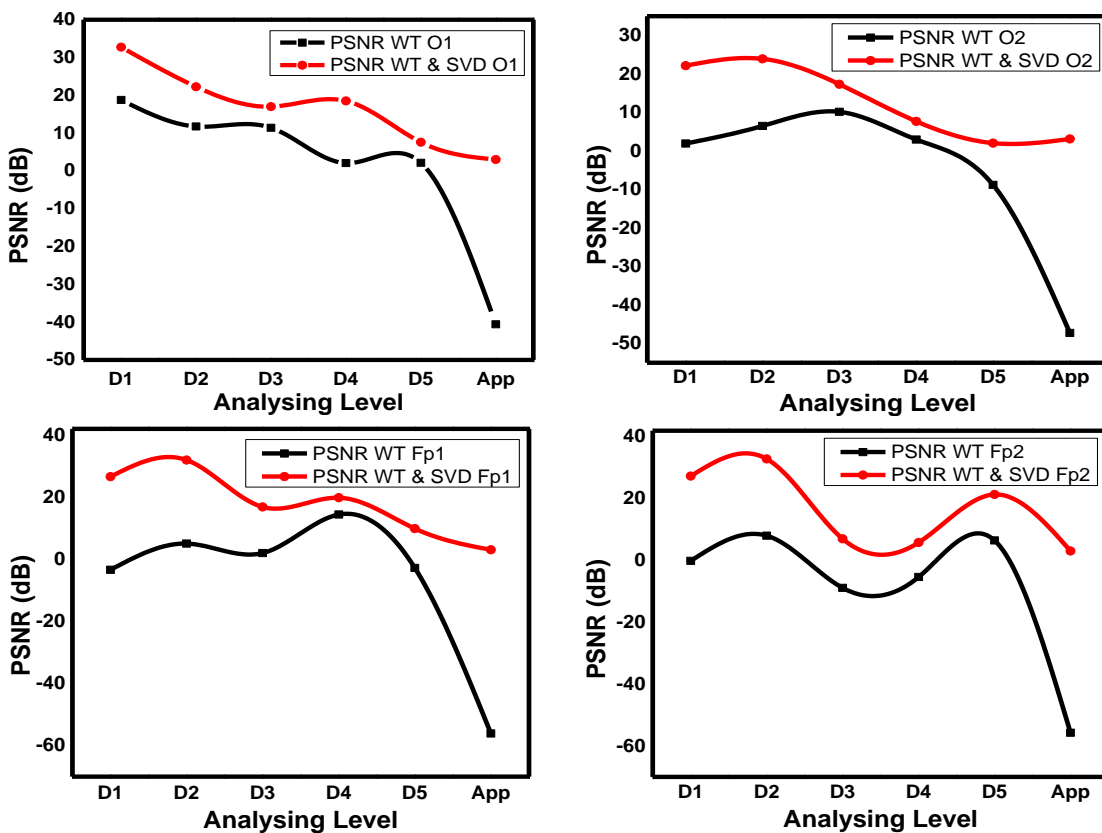


Figure 8. Comparison between discrete wavelet transform and combination of wavelet transform and singular value decomposition based on the value of peak signal to noise ratio of the signal

Conclusion

In this paper, a real-time model for transient VEP signal analysis was proposed and verified. The proposed method was implemented by combining DWT and SVD. The study aimed to accurately pick up EEG signal from the brain, extract VEP response from the background noise, and decompose VEP signals to different frequency band groups, and finally, classify frequency bands by using SVD. MATLAB algorithm was written to calculate the grand average and extract VEP signal. DWT was employed to decompose signals into different frequency bands. SVD verified results of DWT and gave a singular value for each frequency band. PSNRs were used to track the impact of the proposed method. Visual and quantitative results of combined techniques (DWT and SVD) were superior to those produced from the use of each technique individually.

Acknowledgment

The authors would like to thank the Department of Medical Physics, College of Science, Al-Karkh University of Science for their unlimited support. This research was supported by a grant from Universiti Teknologi Malaysia (QJ130000.2526.07H93).

References

1. Başar E. EEG-brain dynamics: relation between EEG and brain evoked potentials. Elsevier-North-Holland Biomedical Press. 1980.
2. Galloway N. Human brain electrophysiology: Evoked potentials and evoked magnetic fields in science and medicine. The British Journal of Ophthalmology. 1990;74(4):255.
3. Almurshed AFH, Ismail AK. Measure Projection Analysis of VEP localization neuron generator. 2015 International Conference on BioSignal Analysis, Processing and Systems (ICBAPS), 2015 International Conference on 2015 May 26 (pp. 108-111). IEEE.
4. Quiroga RQ, Basar E, Schürmann M, Urman MS. Phase-Locking Of Event-Related Alpha Oscillations. 2000.
5. Quiroga R. Obtaining single stimulus evoked potentials with wavelet denoising. Physica D: Nonlinear Phenomena. 2000;145(3):278-92.
6. Almurshed A, Ismail AK. Puzzle task ERP response: time-frequency and source localization analysis. Translational Neuroscience. 2015;6(1):187-97. Doi:10.1515/tnci-2015-0020.
7. Grossmann A, Morlet J. Decomposition of Hardy functions into square integrable wavelets of constant shape. SIAM journal on mathematical analysis. 1984;15(4):723-36.
8. Bertrand O, Bohorquez J, Pernier J. Time-frequency digital filtering based on an invertible wavelet transform: an application to evoked potentials. IEEE

- Transactions on Biomedical Engineering. 1994;41(1):77-88.
9. Demiralp T, Ademoglu A, Schürmann M, Basar-Eroglu C, Basar E. Detection of P300 waves in single trials by the wavelet transform (WT). Brain and language. 1999;66(1):108-28.
 10. Schiff SJ, Aldroubi A, Unser M, Sato S. Fast wavelet transformation of EEG. Electroencephalography and Clinical Neurophysiology. 1994;91(6):442-55.
 11. Almurshed A, Ismail AK. Signal Refinement: Principal Component Analysis and Wavelet Transform of Visual Evoked Response. Research Journal of Applied Sciences, Engineering and Technology. 2015;9(2):106-12.
 12. Gurley K, Kijewski T, Kareem A. First-and higher-order correlation detection using wavelet transforms. Journal of engineering mechanics. 2003;129(2):188-201.
 13. Blankertz B, Dornhege G, Krauledat M, Muller K, Kunzmann V, Losch F. The Berlin brain-computer interface: EEG-based communication without subject training. IEEE Trans Neural Syst Rehabil Eng. 2006;14(2):147-52. DOI:10.1109/TNSRE.2006.875557.
 14. Zhan XD, Kang T, Choi HR. An approach for pattern recognition of hand activities based on EEG and fuzzy neural network. Journal of mechanical science and technology. 2005;19(1):87-96.
 15. Zhang X, Diao W, Cheng Z. Wavelet transform and singular value decomposition of EEG signal for pattern recognition of complicated hand activities. Digital Human Modeling. Springer; 2007. 294-303.
 16. Liu Y, Sourina O, Nguyen MK. Real-time EEG-based human emotion recognition and visualization. Cyberworlds (CW), 2010 International Conference on; 2010: IEEE.
 17. Liu Y, Sourina O, Nguyen MK. Real-time EEG-based emotion recognition and its applications. Transactions on computational science XII. Springer; 2011. 256-77.
 18. Mackay AM, Bradnam MS, Hamilton R, Elliot AT, Dutton GN. Real-time rapid acuity assessment using VEPs: development and validation of the step VEP technique. Investigative ophthalmology & visual science. 2008;49(1):438-41. DOI:10.1167/iovs.06-0944.
 19. Al-maqtari MT, Taha Z, Moghavvemi M. Steady state-VEP based BCI for control gripping of a robotic hand. InTechnical Postgraduates (TECHPOS), 2009 International Conference for 2009 Dec 14 (pp. 1-3). IEEE.
 20. Guger C, Allison BZ, Grosswindhager B, Pruckl R, Hintermuller C, Kapeller C, et al. How Many People Could Use an SSVEP BCI? Frontiers in neuroscience. 2012;6:169. DOI:10.3389/fnins.2012.00169.
 21. Samar VJ, Swartz KP, Raghubeer MR. Multiresolution analysis of event-related potentials by wavelet decomposition. Brain and cognition. 1995;27(3):398-438. DOI:10.1006/brcg.1995.1028.
 22. Nakos G, Joyner D. Linear algebra with applications. Brooks/Cole Publishing Company; 1998.
 23. Hassanpour H, Mesbah M, Boashash B. Time-frequency feature extraction of newborn EEG seizure using SVD-based techniques. EURASIP Journal on Applied Signal Processing. 2004;2004:2544-54.
 24. Odom JV, Bach M, Barber C, Brigell M, Marmor MF, Tormene AP, et al. Visual evoked potentials standard. Documenta ophthalmologica. 2004;108(2):115-23.
 25. Odom JV, Bach M, Brigell M, Holder GE, McCulloch DL, Tormene AP. ISCEV standard for clinical visual evoked potentials. Documenta ophthalmologica. 2010;120(1):111-9.
 26. Kurita-Tashima S, Tobimatsu S, Nakayama-Hiromatsu M, Kato M. The neurophysiologic significance of frontal negativity in pattern-reversal visual-evoked potentials. Investigative ophthalmology & visual science. 1992;33(8):2423-8.
 27. Foxe JJ, Simpson GV. Flow of activation from V1 to frontal cortex in humans. Experimental Brain Research. 2002;142(1):139-50.
 28. Ocak H. Automatic detection of epileptic seizures in EEG using discrete wavelet transform and approximate entropy. Expert Systems with Applications. 2009;36:2027-36. DOI:10.1016/j.eswa.2007.12.065.
 29. Jahankhani P, Kodogiannis V, Revett K. EEG Signal Classification Using Wavelet Feature Extraction and Neural Networks. Modern Computing, 2006. JVA '06. IEEE John Vincent Atanasoff 2006 International Symposium. 2006; 3Oct: 120-4.
 30. Odom JV, Bach M, Brigell M, Holder GE, McCulloch DL, Mizota A, et al. ISCEV standard for clinical visual evoked potentials. Documenta Ophthalmologica. 2016;133(1):1-9. DOI:10.1007/s10633-016-9553-y.